

Influence of drying temperature on the migration of cesium chloride initially dissolved in the liquid water of sugi (*Cryptomeria japonica* D. Don) sapwood

メタデータ	言語: eng 出版者: 公開日: 2016-07-06 キーワード (Ja): キーワード (En): 作成者: Tanaka, Takashi, Murakami, Kaori, Kumata, Atsushi, Kawai, Yasuo メールアドレス: 所属:
URL	http://hdl.handle.net/10297/9725

Influence of drying temperature on the migration of cesium chloride initially dissolved in the liquid water of sugi (*Cryptomeria japonica* D. Don) sapwood

5 Takashi Tanaka^{1*}, Kaori Murakami², Atsushi Kumata³, Yasuo Kawai⁴

¹Graduate School of Agriculture, Shizuoka University, Japan

²Fukushima Prefectural Forestry Research Centre, Japan

³Fukushima Prefectural Ken-nan Agriculture and Forestry Office, Japan

⁴Institute of Wood Technology, Akita Prefectural University, Japan

10

*Corresponding author.

Phone. +81-54-238-4860

Fax. +81-54-238-4860

attanak@ipc.shizuoka.ac.jp

15

Part of this article was presented at the 63rd Annual Meeting of the Japan Wood Research Society, Morioka, Japan, March 2013

20

Abstract: A method with potential utility in radiocesium decontamination from timber harvested in Fukushima region, where fallout from the Fukushima Daiichi nuclear disaster was deposited, involves drying the timber and planing away the contaminated wood. The objective of this study was to investigate the influence of drying temperature on the migration of cesium dissolved in the liquid water of sugi (*Cryptomeria japonica* D. Don) sapwood during the drying process. Small specimens of sugi sapwood impregnated with aqueous cesium chloride (CsCl) solution were dried at 20 °C or 90 °C, and the migration of CsCl during drying was examined by

25 means of X-ray imaging. The results of this study indicate that the drying of sugi sapwood at any temperature causes surface accumulation of dissolved cesium, which is affected by both the drying temperature and grain orientation of the surface. Statistical analysis confirmed that a high drying temperature causes greater surface accumulation of CsCl during drying. We recommend using higher temperatures to dry sugi sapwood when

25

30

Keywords: cesium chloride (CsCl), drying temperature, Japanese cedar, redistribution during drying, X-ray imaging

Introduction

Radiocesium contamination of forest and forest products after the Fukushima Daiichi nuclear disaster in March 2011 remains an environmental concern in Japan. Fallout radiocesium entered trees of the surrounding regions through direct deposition of atmospheric radiocesium onto tree surfaces and uptake from the soil via the roots (Hasegawa et al. 2009). Radiocesium is therefore detected not only in the bark but also in sapwood and heartwood (Kuroda et al. 2013). Approximately 50–90% of radiocesium in aerosols is water soluble (Tanaka et al. 2013) and thus is partly dissolved in the tree sap.

A brown discoloration (kiln brown stain), which causes quality defects, often develops approximately 1 mm under the timber surface after kiln drying (Kreber and Haslett 1997). This discoloration is attributed to a kiln-drying-induced gradient of soluble nitrogenous or carbohydrate compounds from the inside to the surface (King et al. 1974, Terziev et al. 1993, Theander et al. 1993, Terziev 1995). Based on a simulation with a percolation model, Salin (2008a) demonstrated that kiln brown stain results from the accumulation of a discoloration-inducing substance dissolved in the liquid water of sapwood indicating that the movement of free water in wood during drying causes the migration of dissolved substances from the inside to the surface. Tanaka and Kawai (2014) conducted the drying experiment with small sugi specimens soaked with a CsCl solution, and used X-ray imaging to visualize the inside-to-surface migration of dissolved CsCl in the liquid water of the wood. Their data indicate that CsCl initially dissolved in the liquid water of wood migrates from inside to the surface during the kiln drying of 65°C especially in sapwood. Thus, the concentration of CsCl inside samples seems to have decreased by half after the sapwood is dried. These results suggest that drying and planing the timber,

especially sapwood, harvested in the Fukushima regions before commercialization can successfully decontaminate it of radiocesium. Fortunately, the radiocesium concentration in heartwood is lesser than that in sapwood (Kuroda *et al.* 2013). Thus, we consider that this method has potential for the decontamination of sawn timber in Fukushima.

5 Kreber and Haslett (1997) have reported that the formation of kiln brown stain is intensified with a higher drying temperature. Given that radiocesium in wood exhibits a similar migratory behavior, lumber decontamination by drying and planing should become more efficient with a higher drying temperature. Thus, the objective of this study was to investigate the influence of drying temperature on the migration of CsCl in the liquid water of sugi sapwood during drying. To this purpose, sugi sapwood impregnated with CsCl aqueous
10 solution was dried at different temperatures, and the migration of CsCl was observed by means of X-ray imaging. The distribution of CsCl in wood samples was evaluated at the end of drying and the effect of drying temperature on the formation of surface deposition during drying was statistically analyzed.

Materials and methods

15 Twelve sugi (*Cryptomeria japonica*) sapwood samples with dimensions of $15 \times 15 \times 15 \text{ mm}^3$ (R \times T \times L) were cut from three air-dried tree trunks (Table 1) with a circular table saw. Six samples were soaked in an aqueous solution of 3% CsCl, and the other six were soaked in distilled water (control samples). The samples were intermittently exposed to lower pressure (10 kPa) to saturate them with the solutions. The saturated samples were then softly wiped with cleaning tissues.

An X-ray machine (SR-1010, Softex Co., Ltd., Ebina, Japan) equipped with a digital X-ray sensor (NX-04H, Softex Co., Ltd., Ebina, Japan) was used to scan the samples from three different directions (40-kVp tube voltage, 14-mA tube current, 1.0-mm-thick aluminum filter). Samples were exposed for 1 s, and the scanned image was saved in the “.dcm” file format at a resolution of 5340×5000 pixels (20 pixel mm^{-1}) in 12-bit (0–4095) grayscale.

Three CsCl-soaked samples and three control samples were then dried in a conditioning chamber at 20°C and 65% relative humidity. The samples were removed from the chamber after 40, 130, 230, 350, 530, and 1410 min of drying, scanned as described above, and then immediately placed back into the chamber. Experiments were stopped after 1410 min of drying, when the weights of samples soaked with distilled water were lower than their corresponding air-dry weights.

The remaining samples were dried in a conditioning chamber at the dry-bulb temperature of 90°C and 26% relative humidity (60°C wet-bulb temperature). The samples were removed from the chamber after 10, 25, 40, 60, 85, and 125 min of drying, scanned as described before, and then immediately placed back into the chamber. Experiments were stopped after 125 min of drying, when the weights of samples soaked with distilled water were lower than their air-dry weights.

Equation 1, which was derived experimentally from 14 poly(methyl methacrylate) (PMMA) plates of various thicknesses (1.0–30 mm) by Tanaka and Kawai (2014), was used to calculate PMMA-equivalent-thickness distributions (PMMA-ET_HD, y) to the brightness value (x) for all X-ray images.

$$y = -26.65 \ln x + 209.12 \quad (\text{Eq. 1})$$

The PMMA-ETHD value before soaking was subtracted from the corresponding value after drying to calculate the net change in PMMA-ETHD. To avoid sample deformation during drying, images were registered in ImageJ 1.45s (Wayne Rasband, National Institute of Health, USA) and its extension bUnwarpJ 2.6 (Ignacio Arganda-Carreras, Massachusetts Institute of Technology) before subtracting. Because Cs attenuates X-rays 90-fold more strongly than water (Hubbell and Seltzer 2004, Ida 2008), changes in the PMMA-ETHD predominantly reflect the concentration distribution of deposited CsCl. To compare the concentration distribution of deposited CsCl with that of the initially dissolved CsCl, the PMMA-ETHD in each pixel was divided by the average value of the change in PMMA-ETHD.

To determine whether the drying temperature affected the average surface CsCl concentration, analysis of variance (ANOVA) was conducted on the average CsCl concentrations at 0–1 mm below the surface obtained at three different drying temperatures, 20°C, 65°C, and 90°C, each consisting of three data points (three specimens). The 65 °C data points were extracted from the original data of the previous study (Tanaka and Kawai 2014).

Results and discussion

Figure 1 shows the X-ray images of the tangential surface of the samples during drying. As expected, a sharp contrast between the surface and subsurface of wood gradually developed during drying in the samples soaked with CsCl solution in both the drying conditions. On the other hand, no contrast developed between the surface and subsurface in samples soaked with distilled water, indicating that the substance providing X-ray contrast was CsCl. These results are consistent with those of the previous study (Tanaka and Kawai 2014),

confirming that the drying of sugi sapwood at any temperature causes the surface accumulation of dissolved CsCl during drying.

Figure 2 shows the changes of brightness profiles (over the lines T₁, L₁, T₂ and L₂ drawn in Figure 1) during drying in the control samples, which indicated no significant differences between drying at 20 °C and 90 °C in the formation or change of a brightness profile during the process. This suggests that the drying temperature has no significant impact on how liquid water moves in sugi sapwood during drying, except for the total amount of drying time required. Interestingly, we demonstrated a phenomenon in which the liquid water at the center part of the sample decreased more rapidly than that in the other parts, thereby producing a double-peak in the water distribution along the lines L₁ and L₂ in Figure 2 during drying. Although it is well known that sapwood drying above the fiber saturation point is usually gradient-free (Wiberg 1995, Wiberg and Morén 1999), to the best of our knowledge, the “inverse gradient” drying observed in the present study has not been reported before. Further investigation is needed to elucidate this phenomenon. On the other hand, for samples soaked with a CsCl aqueous solution, drying at 90 °C caused a greater difference in brightness between the surface and subsurface at the end of drying (Fig. 3). This result indicates that drying at 90 °C enhanced the migration of CsCl from the inside to the surface of sugi sapwood.

We also analyzed the relative concentration distribution of CsCl in samples at the end of the drying process compared to that of initially dissolved CsCl (Figure 4). Overall, 90 °C drying showed a broader distribution of CsCl accumulation (> 300% concentration increase, as indicated in red in the heat maps; Fig. 4). This indicates that the higher drying temperature intensified the accumulation of CsCl just below the surface.

This is in agreement with the finding that kiln brown stain formation is also intensified with a higher drying temperature (Kreber and Haslett 1997).

Figure 5 illustrates the relationship between drying temperature and relative CsCl concentration in the 1-mm-thick surface layers, which were calculated by determining average CsCl concentrations at 0–1 mm below the surface (Figure 4). The 65 °C data points included in the figure are extracted from the original data of the previous report (Tanaka and Kawai 2014). In tangential surfaces, the surface accumulation of CsCl developed similarly regardless of drying temperature. By contrast, the surface accumulation of CsCl at 65 °C drying was minimum in radial surfaces, whereas maximum in cross-sectional surfaces. These results indicate that the grain direction affects the variation of the surface accumulation of CsCl with the increased drying temperature. One reason for this directionality could be the quite low permeability of sugi in the radial direction. Indeed, considering that sugi is one of the least radially permeable softwoods (Tanaka et al. 2015), different results may be observed in other species. In addition, green sugi wood has fewer aspirated pits (Matsumura et al. 2005) than dried sugi wood; therefore, the drying of green sugi sapwood may also lead to a different outcome (presumably to more migration in the radial direction).

The average CsCl concentration of all surfaces increased as the drying temperature increased, which was calculated by averaging the three data points (tangential, radial, and cross-section surfaces) shown in Figure 5. To determine whether the drying temperature affected the average surface CsCl concentration, ANOVA was performed between the three temperature groups 20°C, 65°C, and 90°C, each consisting of three data points (three specimens). The calculated F value (Table 2) was larger than the 5% significance level threshold value

5.143, indicating that the average relative CsCl concentration was significantly ($p < 0.05$) influenced by the drying temperature. These results shown in Figure 5 and Table 2 support the idea that a higher drying temperature intensifies the surface accumulation of CsCl initially dissolved in liquid water in sugi sapwood.

Considering the concentration of CsCl inside samples reduced to approximately 50% of the initial CsCl

5 concentration by the kiln drying at 65°C (Tanaka and Kawai 2014), a drying temperature higher than 65°C may achieve the removal of more than 50% CsCl after drying and planing. A possible mechanism for this phenomenon involves the lower surface tension of liquid water at higher temperatures, which allows liquid water to migrate against capillary forces in tracheids.

When modeling the surface accumulation of dissolved substances during drying, more accurate data can
10 be obtained by taking into account the drying temperature, in addition to pore-network and percolation processes (Salin 2006a, Salin 2006b, Salin 2008a) and physical damage to the surface layers (Salin 2008b).

The findings of this study are encouraging for the success of using drying and planing of Fukushima-sourced timber as a method of radiocesium decontamination, in that a higher temperature drying process presumably increase the amount of radiocesium removed during planing. However, our study findings
15 reflect cubic wood specimens. Further investigation is needed to clarify the influence of the shape of sawn timber on the surface concentration. In fact, our future studies include conducting an experiment with actual size, radiocesium-contaminated timber, while utilizing a high temperature drying process.

Conclusions

The results of this study indicate that the drying of sugi sapwood at any temperature causes the surface accumulation of dissolved CsCl during drying, and that both drying temperature and grain direction of the surface affect the degree of surface accumulation. Overall, on all surface averages, a higher drying temperature induced greater surface accumulation of CsCl during drying. Thus, we recommend that when the proposed method of drying and planing of Cs-contaminated timber is to be tried for radiocesium contamination, a suitably high drying temperature should be utilized to improve the process.

Acknowledgments: This work was supported by JSPS KAKENHI Grant Number 24780170 and LIXIL JS Foundation Research Grant No. 12-66. We thank Drs. Katsuhiko Takata and Shigeru Yamauchi at Akita Prefectural University for donating sugi samples and providing CsCl, respectively.

References

- Hasegawa H, Tsukada H, Kawabata H, Chikuchi Y, Takaku Y, Hisamatsu S (2009) Effect of the counter anion of cesium on foliar uptake and translocation. *J Environ Radioactivity* 100:54–57
- Hubbell JH, Seltzer SM (2004) Tables of X-Ray Mass Attenuation Coefficients and Mass Energy-Absorption Coefficients (version 1.4), <http://physics.nist.gov/xaamdi>. Accessed 26 June 2012
- 5 Ida T (2008) How to use powder diffraction method (2) – Preparation of Specimen – (in Japanese). *J Flux Growth* 3:2–6
- King B, Oxley TA, Long KD (1974) Soluble nitrogen in wood and its redistribution on drying. *Material Organismen* 9:241–254
- 10 Kreber B, Haslett AN (1997) A study of some factors promoting kiln brown stain formation in radiata pine. *Holz Roh-Werkst* 55:215–220
- Kuroda K, Kagawa A, Tonosaki M (2013) Radiocesium concentrations in the bark, sapwood and heartwood of three tree species collected at Fukushima forests half a year after the Fukushima Dai-ichi nuclear accident. *J Environ Radioactivity* 122:37–42
- 15 Matsumura J, Yamasaki Y, Oda K, Fujisawa Y (2005) Profile of bordered pit aspiration in *Cryptomeria japonica* using confocal laser scanning microscopy: pit aspiration and heartwood color. *J Wood Sci* 51:328–333
- Salin JG (2006a) Modelling of the behaviour of free water in sapwood during drying. Part 1. A new percolation approach. *Wood Mater Sci Eng* 1:4–11
- Salin JG (2006b) Modelling of the behaviour of free water in sapwood during drying. Part 2. Some simulation

results. Wood Mater Sci Eng 1:45–51

Salin JG (2008a) Drying of liquid water in wood as influenced by the capillary fiber network. Drying Technol

26:560–567

Salin JG (2008b) Almost all wooden pieces have a damaged surface layer—Impact on some properties and

5 quality. Proceedings of the European COST Action E53 Conference. Delft, Netherlands, pp. 135–143

Tanaka K, Sakaguchi A, Kanai Y, Tsuruta H, Shinohara A, Takahashi Y (2013) Heterogeneous distribution of

radiocesium in aerosols, soil and particulate matters emitted by the Fukushima Daiichi Nuclear Power

Plant accident: retention of micro-scale heterogeneity during the migration of radiocesium from the air

into ground and river systems. J Radioanal Nucl Chem 295:1927–1937

10 Tanaka T, Kawai Y (2014) Migration of cesium chloride dissolved in the liquid water of sugi (*Cryptomeria*

japonica D. Don) during drying at 65 °C. Holzforschung 68(5): 591–597

Tanaka, T., Kawai, Y., Sadanari, M., Shida, S., Tsuchimoto, T. (2015) Air permeability of sugi (*Cryptomeria*

japonica) wood in the three directions. Maderas. Ciencia y Tecnología 17(1), 17–28

Terziev N, Boutelje J, Söderström O (1993) The influence of drying schedules on the redistribution of

15 low-molecular sugars in *Pinus sylvestris* L. Holzforschung 47:3–8

Terziev N (1995) Migration of low-molecular sugars and nitrogenous compounds in *Pinus sylvestris* L. during

kiln and air drying. Holzforschung 49:565–574

Theander O, Bjurman J, Boutelje JB (1993) Increase in the content of low-molecular carbohydrates at lumber

surfaces during drying and correlations with nitrogen content, yellowing and mould growth. Wood Sci

Technol 27:381–389

Wiberg P (1995) Moisture distribution changes during drying. Holz Roh- Werkst 53:402

Wiberg P, Morén TJ (1999) Moisture flux determination in wood during drying above fibre saturation point using CT-scanning and digital image processing. Holz Roh-Werkst 57:137–144

5

Table 1. Density and number of annual rings of the testing samples of different origins.

Tree and tree origin	Sample no.	Density at (20 °C, 65% RH)	Number of annual rings	Solution for soaking	Drying temperature and relative humidity
Tree 1 ^a	1s_Cs20	0.39	7	CsCl aq. sol.	20 °C, 65%
	1s_w20	0.40	7	Distilled water	
	1s_Cs90	0.43	9	CsCl aq. sol.	90 °C, 26%
	1s_w90	0.42	9	Distilled water	(Wet-bulb temperature: 60 °C)
Tree 2 ^a	2s_Cs20	0.42	8	CsCl aq. sol.	20 °C, 65%
	2s_w20	0.42	7	Distilled water	
	2s_Cs90	0.38	9	CsCl aq. sol.	90 °C, 26%
	2s_w90	0.40	7	Distilled water	(Wet-bulb temperature: 60°C)
Tree 3 ^a	3s_Cs20	0.36	6	CsCl aq. sol.	20 °C, 65%
	3s_w20	0.42	6	Distilled water	
	3s_Cs90	0.39	5	CsCl aq. sol.	90 °C, 26%
	3s_w90	0.37	5	Distilled water	(Wet-bulb temperature: 60 °C)

^a Semboku, Akita prefecture (plantation forest), approximately 50 year old trees.

Table 2. ANOVA of the relationship between drying temperature and relative CsCl concentration in the 1-mm-thick surface layers.

Source of variation	Sum of squares	Degrees of freedom	Mean of squares	F value	Significance level*
Temperature factor (Between-group)	481.4	2	240.7	9.408 >	5.143
Error (Within-group)	153.5	6	25.6		
Total	634.9				

* represents significance level of $p < 0.05$

Figure captions

Fig. 1 X-ray images of tangential surfaces of the testing samples during drying. The vertical and horizontal directions of each image represent the longitudinal and tangential directions of each sample, respectively. The white lines (T_{1-4} , L_{1-4}) represent the tangential (T) and longitudinal (L) lines over which brightness profiles were measured

Fig. 2 Changes in brightness profiles along lines T_1 , L_1 , T_2 and L_2 in Figure 1 (samples soaked with distilled water) during drying at 20 and 90°C

Fig. 3 Changes in brightness profiles along lines T_3 , L_3 , T_4 and L_4 in Figure 1 (samples soaked with a CsCl solution) during drying at 20 and 90°C

Fig. 4 Relative CsCl concentrations at the end of drying at 20 °C and 90 °C compared with initial CsCl concentrations, with the heat map describing more intense concentrations of CsCl deposition at the red end of the provided spectrum

Fig. 5 Relationship between drying temperature and relative CsCl concentration in the 1-mm-thick surface layers.

^a indicates data points from the previous study by Tanaka and Kawai (2014)

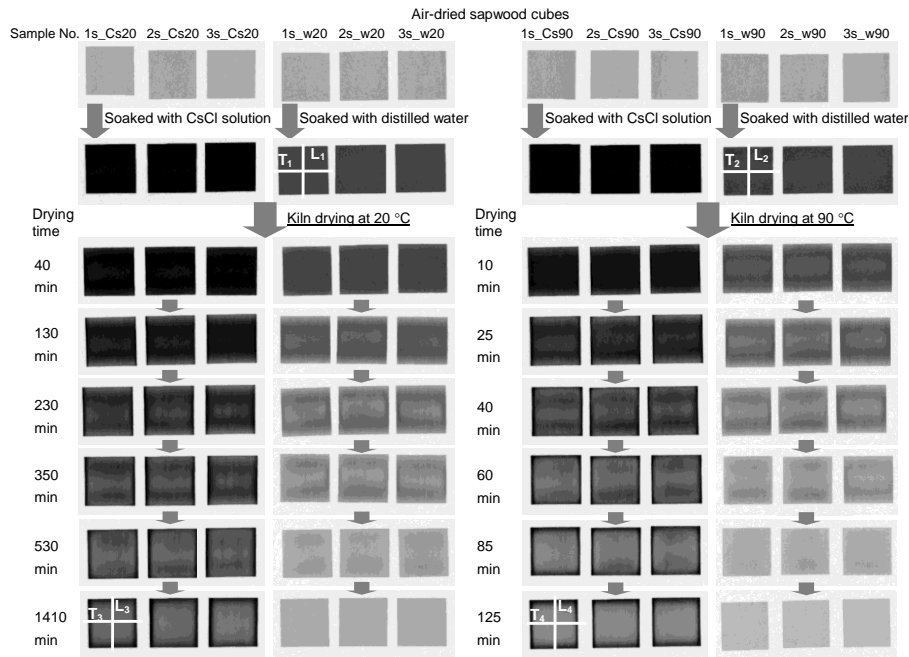


Fig. 1 X-ray images of tangential surfaces of the testing samples during drying. The vertical and horizontal directions of each image represent the longitudinal and tangential directions of each sample, respectively. The white lines (T₁₋₄, L₁₋₄) represent the tangential (T) and longitudinal (L) lines over which brightness profiles were measured

5

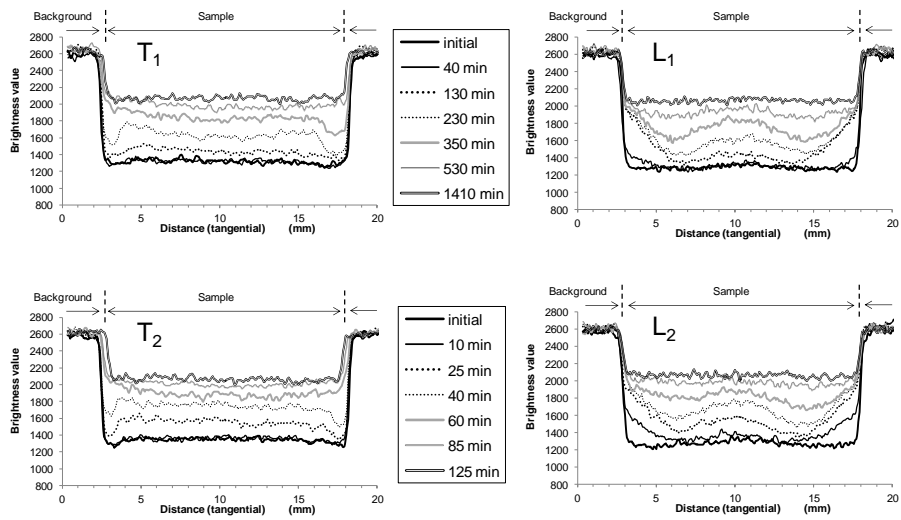


Fig. 2 Changes in brightness profiles along lines T₁, L₁, T₂ and L₂ in Figure 1 (samples soaked with distilled water) during drying at 20 and 90°C

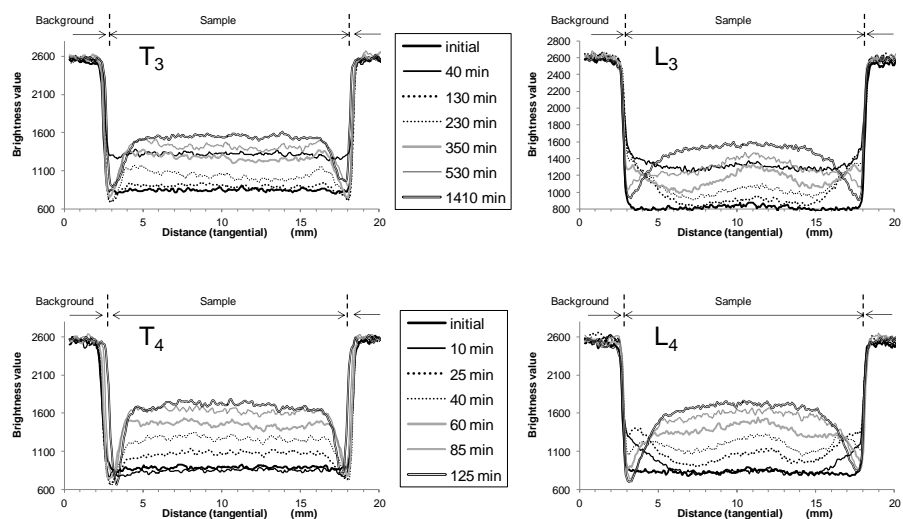


Fig. 3 Changes in brightness profiles along lines T₃, L₃, T₄ and L₄ in Figure 1 (samples soaked with a CsCl solution) during drying at 20 and 90°C

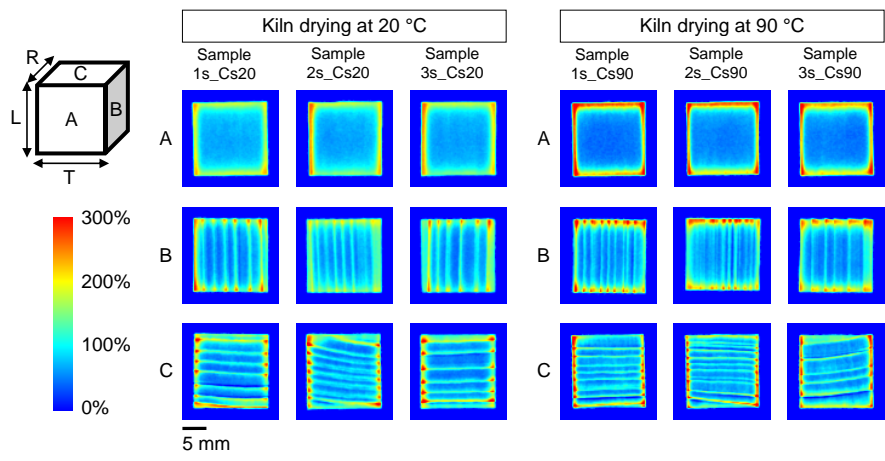


Fig. 4 Relative CsCl concentrations at the end of drying at 20 °C and 90 °C compared with initial CsCl concentrations, with the heat map describing more intense concentrations of CsCl deposition at the red end of the provided spectrum

5

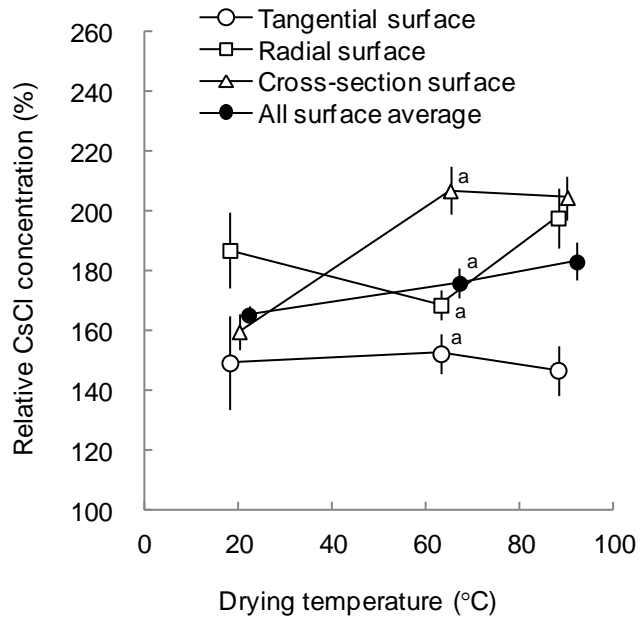


Fig. 5 Relationship between drying temperature and relative CsCl concentration in the 1-mm-thick surface layers.

^a indicates data points from the previous study by Tanaka and Kawai (2014)